International Journal of Pharmaceutics 409 (2011) 137–149

Contents lists available at ScienceDirect

International Journal of Pharmaceutics

journal homepage: www.elsevier.com/locate/ijpharm

Modeling the motion and orientation of various pharmaceutical tablet shapes in a film coating pan using DEM

William R. Ketterhagen*

Pfizer Global Research and Development, Eastern Point Road, MS 8156-001, Groton, CT 06340, USA

ARTICLE INFO

Article history:
Received 30 November 2010
Received in revised form 4 February 2011
Accepted 21 February 2011
Available online 26 February 2011

Keywords:
Tablet shape
Film coating
Coating uniformity
Discrete element method
Quality by Design (QbD)

ABSTRACT

Film coating uniformity is an important quality attribute of pharmaceutical tablets. Large variability in coating thickness can limit process efficiency or cause significant variation in the amount or delivery rate of the active pharmaceutical ingredient to the patient. In this work, the discrete element method (DEM) is used to computationally model the motion and orientation of several novel pharmaceutical tablet shapes in a film coating pan in order to predict coating uniformity. The model predictions are first confirmed with experimental data obtained from an equivalent film coating pan using a machine vision system. The model is then applied to predict coating uniformity for various tablet shapes, pan speeds, and pan loadings. The relative effects of these parameters on both inter- and intra-tablet film coating uniformity are assessed. The DEM results show intra-tablet coating uniformity is strongly influenced by tablet shape, and the extent of this can be predicted by a measure of the tablet shape. The tablet shape is shown to have little effect on the mixing of tablets, and thus, the inter-tablet coating uniformity. The pan rotation speed and pan loading are shown to have a small effect on intra-tablet coating uniformity but a more significant impact on inter-tablet uniformity. These results demonstrate the usefulness of modeling in guiding drug product development decisions such as selection of tablet shape and process operating conditions.

1. Introduction

Pharmaceutical tablets are often spray-coated with a cosmetic or functional film coating in the manufacture process. Cosmetic coatings are applied to immediate release tablets and may be applied for one or more of the following reasons: to improve taste masking, dose differentiation, tablet elegance, and others. Functional coatings are applied to modify the release rate of the active drug substance from the tablet for controlled release applications. This approach may be taken to reduce adverse events, improve pharmacokinetic profiles, or reduce dosing frequency to improve patient compliance and/or convenience. Finally, in some instances, the coating may contain an active pharmaceutical ingredient.

The uniformity of the film coating – whether cosmetic or functional – is an important quality attribute. In the case of cosmetic coatings, poor coating uniformity, or large variability in coating thickness, reduces process efficiency as the process must be run for longer times to ensure that all tablets have attained the desired level of coating thickness. In the case of functional coatings, attaining a uniform coating is even more important. Here, significant variability in coating thickness between tablets can dramatically affect the lag time and/or release rate between these tablets.

There are two different types of film coating uniformity to consider. First, inter-tablet coating uniformity describes the level of uniformity between different tablets. Second, intra-tablet coating uniformity describes the level of uniformity between different sides of a given tablet. In general, the level of inter-tablet uniformity depends on the tablet mixing dynamics which govern the distribution of tablet appearances in the spray zone. On the other hand, intra-tablet coating uniformity depends on the orientation of tablets as they move through the spray zone. If a preferred tablet orientation exists as tablets move through the spray zone, the intra-tablet coating uniformity may be poor. Both the tablet mixing dynamics and tablet orientation may be driven by (1) tablet properties such as size and shape, (2) process parameters such as pan speed, pan loading, and (3) the size and geometry of the pan and any internal features such as baffles.

Inter-tablet film coating uniformity is closely tied to the distributions of the coating mass gain per pass through the spray zone and the circulation time between consecutive appearances in the spray zone. Mann et al. (1979) and Mann (1983) have shown that inter-tablet coating variability, given by the coefficient of variation, CoV_{inter}, is governed by the distributions of coating mass per pass and tablet circulation time as well as the total coating time, t, as:

$$CoV_{inter} = \sqrt{\left(\frac{\sigma_m}{\mu_m}\right)^2 \frac{\mu_{ct}}{t} + \left(\frac{\sigma_{ct}}{\mu_{ct}}\right)^2 \frac{\mu_{ct}}{t}} \quad (1)$$

* Tel.: +1 860 686 2868; fax: +1 860 686 7521.
E-mail address: william.ketterhagen@pfizer.com

0378-5173/$ – see front matter © 2011 Elsevier B.V. All rights reserved.
doi:10.1016/j.ijpharm.2011.02.045

where μ and σ are the mean and standard deviation, respectively, and the subscripts m and ct refer coating mass per pass and circulation time, respectively. Thus, by determining the statistics of these two distributions, inter-tablet uniformity can be quantified. Generally, the wider either distribution is, the greater the inter-tablet film coating variability. Following an approach used by several other researchers (Kalbag et al., 2008; Leaver et al., 1985; Pandey et al., 2005; Sandadi et al., 2004; Yamane et al., 1995), the residence time in the spray zone per pass is used in this work as a proxy for the coating mass gain per pass. There is not an analogous theory for intra-tablet coating uniformity. Rather, good intra-tablet uniformity is dependent on maintaining a relatively uniform distribution of tablet orientations as they pass through the spray zone.

The residence time and circulation time distributions have been recently studied with both experimental and computational approaches, and many of the key results have been succinctly summarized by Kalbag et al. (2008) and Kalbag and Wassgren (2009). The findings have generally shown that the mean value of the residence time per pass decreases with either increasing pan speed or pan loading (Kalbag et al., 2008; Leaver et al., 1985; Mueller and Kleinebudde, 2007; Pandey et al., 2005; Sandadi et al., 2004). Additionally, some have reported that the standard deviation of the residence time per pass also decreases with either increasing pan speed or pan loading (Leaver et al., 1985; Yamane et al., 1995). Several researchers have also observed that the mean circulation time decreases with increasing pan speed or decreasing pan loading (Leaver et al., 1985; Pandey et al., 2005; Sandadi et al., 2004; Yamane et al., 1995). Some have also reported that the standard deviation of the circulation time decreases with increasing pan speed (Pandey et al., 2005; Yamane et al., 1995). However, no data has been reported on the effect of pan loading on the standard deviation. It is difficult to use Eq. (1) to discern the trends in CoV_{inter} based solely on the qualitative results summarized above. However, experimental observations have shown that improved inter-tablet coating uniformity is achieved for increased pan speeds (Leaver et al., 1985; Rege et al., 2002; Tobiska and Kleinebudde, 2003a) and decreased pan loading (Mancoff, 1998; Skultety et al., 1988).

Further, recent papers by Turton (2008, 2010) have reviewed the current state of the art in modeling of film coating processes and coating uniformity. Several different approaches ranging from phenomenological models to more computationally intensive DEM models have been developed. Some examples of these approaches include a surface renewal model (Denis et al., 2003) in which the tablet bed is subdivided into an active spraying region and a drying/mixing region. That model was used to predict the evolution of coating mass distribution over time; however, the authors did not specifically determine inter-tablet coating uniformity. Further, experimental data was required to fit the model parameters. Monte Carlo approaches have also been developed to examine inter-tablet (Pandey et al., 2006a) and intra-tablet (Freireich et al., 2011; Freireich and Wassgren, 2010) coating uniformity in pan coaters. These approaches also rely on probability distributions determined either experimentally or with a DEM modeling approach. Finally, analytical approaches such as that of Kalbag and Wassgren (2009) seek to determine inter-tablet coating uniformity as a function of several process parameters. That model successfully predicted the trends in coating uniformity, but again, experimental data was required to determine the constants in the model that were specific to the system of interest (e.g. coating pan geometry).

Despite the fair amount of work in this area, only a limited amount of work addresses the topic of tablet shape and its impact on either inter- or intra-tablet coating variability. Frequently, experimental studies focus on just one tablet shape such as oval (Tobiska and Kleinebudde, 2003a), standard round concave (SRC) (Ho et al., 2007; Leaver et al., 1985; Perez-Ramos et al., 2005; Sandadi et al., 2004), or spherical (Chang and Leonzio, 1995) while computational approaches that directly represent tablet shape (i.e. DEM models) (Kalbag and Wassgren, 2009; Kalbag et al., 2008; Pandey et al., 2006b; Yamane et al., 1995) usually assume a spherical tablet shape to reduce the computational demand. There are a few exceptions that have investigated tablet shape as described in the following paragraphs.

Wilson and Crossman (1997) performed film coating experiments to examine the effect of four different tablet shapes (round, capsule, small and large oval) and pan speed on intra-tablet coating uniformity. They observed that the round tablets had the best intra-tablet uniformity while the worst, the large oval, had significant variability. The tablet band and edge of the land only had approximately 50% the coating thickness of that on the tablet face. The pan speed was found to significantly affect the level of coating on the bands of the tablets, but had little effect on the coating levels on the tablet faces or edges. They also concluded that tablets closer to a spherical shape are likely to have a less variability in the coating thickness. Experimental data from other researchers has shown the tablet faces to have as much as a 30% thicker coating on the tablet face as compared to the tablet band (Ho et al., 2007; Perez-Ramos et al., 2005), but this work only examined SRC tablet shapes. More recently, Freireich and Wassgren (2010) developed a theoretical model and used Monte Carlo simulations to predict intra-tablet coating uniformity. While their analysis only considered spherical particles, they showed that by constraining the spheres to a preferred orientation in the spray zone, the intra-tablet coating variability is increased. That approach has been recently extended (Freireich et al., 2011) by applying the Monte Carlo analysis to the DEM data generated in the present work for five non-spherical tablet shapes. The Monte Carlo simulations permit the calculation of the asymptotic coefficient of variation of intra-tablet coating thickness, CoV_{intra}, after several thousand appearances in the spray zone – far longer than is attainable in current DEM simulations. Due to their preferred orientation in the spray zone, the CoV_{intra} for the non-spherical tablets was shown to be greater than that for spheres.

Other experimental approaches focused their efforts on monitoring tablet movements in the coating pan, often using a machine vision system in place of the spraying system. Sandadi et al. (2004) used a machine vision system to study tablet mixing in terms of circulation time and a surface time (or residence time within the spray zone) for three different sizes of SRC tablets at varying process conditions. Later, Pandey et al. (2005) compared the movement of these SRC tablets with spherical particles and found no significant differences in mean circulation or surface times between the two shapes. Pandey et al. (2006b) then used a DEM model to predict the dynamic angle of repose and surface velocities of spherical particles and compared the results to previous DEM results (Yamane et al., 1998) and experimental data (Pandey et al., 2005). Both qualitative and, in some cases quantitative, agreement was observed with the differences being attributed to the 'wavy' shape of the free surface which was more prominent in the experiments than in the simulations.

Researchers have increasingly begun to incorporate non-spherical particle shapes into DEM models with several techniques reported (Džiugys and Peters, 2001; Hogue, 1998). Two of the more common techniques include directly modeling a given shape (e.g. ellipsoid or superquadrics) or using the "glued sphere" approach where constituent spheres are rigidly glued together to form a specified shape. Two cases directly applicable to pharmaceutical tablets include an SRC shaped tablet reported by Song et al. (2006) and flat-faced tablets (i.e. cylinders) reported by Kodam et al. (2010a,b). While these approaches model the shape of a tablet exactly, there is significant overhead in developing the contact detection routines. The current work uses the glued sphere approach which, while

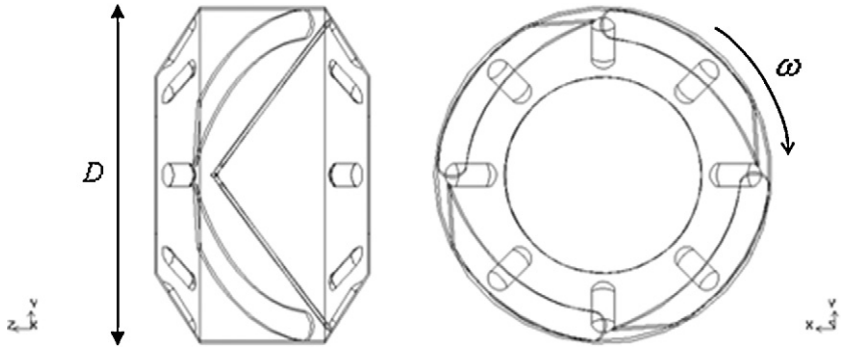

Fig. 1. Diagram of the modeled film coating pan.

losing some accuracy in the tablet shape, gains in flexibility to quickly model a wide variety of tablet shapes.

As described above, much of the work investigating film coating uniformity has neglected the effect of tablet shape or assumed spherical tablets to reduce computational demands. The objective of this work is to examine the effect of a wide variety of tablet shapes on inter- and intra-tablet coating uniformity. This assessment is carried out by monitoring the residence time per pass and the circulation time in addition to the orientation of tablets within the spray zone. A secondary objective is to assess the effect of the pan speed and pan load on the inter- and intra-tablet coating uniformity. Additionally, the model predictions are confirmed through comparison with experimental data acquired from a machine vision system installed in a film coating pan of the same dimensions. The advantages of using the DEM approach include the capability to model tablets of arbitrary shape and predict the coating uniformity performance *in silico* to enable both time and cost savings (by avoiding the purchase of tooling, producing tablets, coating tablets, and analyzing the experimental results). Furthermore, the use of DEM permits exploration of the effects of individual process parameters and tablet shape – and compare the relative effects of each – on both inter- and intra-tablet coating uniformity to enable process design and optimization.

2. Experimental details

Experiments to monitor tablet mixing were carried out in a lab-scale Vector (Marion, IA) LDCS 1.5 L film coating pan. The pan diameter was 29.2 cm and the pan internals included four custom-manufactured baffles positioned in an alternating configuration that traversed the length of the pan and eight small, anti-slip bars on each of the conical ends. The motion of a single tracer tablet was observed by a CV-3000 machine vision system (Keyence Corporation, Osaka, Japan), consisting of a video camera and high intensity light installed in place of the spray gun and a system of computer hardware and software to acquire and analyze the signal. The camera recorded images at a rate of 30 frames per second which were analyzed in real-time for the appearance of the tracer tablet. The system recorded the frames in which the tracer was present and how many pixels of target color were detected, indicating how much of the tracer was exposed. These data were subsequently post-processed to determine the relevant statistics which relate to tablet mixing. The camera-to-bed distance was fixed throughout the course of the experiment. Therefore, the camera field of view was also constant and had dimensions of approximately 7.0 cm by 15.2 cm with the long side aligned parallel to the pan axis.

The tablets used in the experiments including the tracer were 15/32″ diameter standard round concave (SRC) tablets. The tablets consisted of 800 mg of a placebo blend of 50% Avicel PH200, 49.9% Lactose FF316, and 0.1% Red Lake. The non-tracer tablets were previously coated with a clear film coat to prevent tablet erosion. The tracer tablet was coated with Opadry II Green (Colorcon, Harleysville, PA) to create significant contrast in color permitting detection of the tracer appearances within the camera field of view. The experiments were run at two different pan loadings, 0.7 kg and 1.0 kg, and at a pan speed of 22 RPM for approximately 30 min. This run time allowed for a sufficient number of tracer tablet appearances (~1300 and 950, respectively) to ensure that statistically representative data was acquired.

3. Computational details

The discrete element method (DEM), initially developed by Cundall and Strack (1979), is used in this work to model the tablet motion in a rotating film coating pan. Since the initial development of DEM, many theoretical advancements have occurred (Zhu et al., 2007). These advancements have led to applications of DEM modeling within the pharmaceutical industry (Ketterhagen et al., 2009) as well as many other areas where particulate systems are present (Zhu et al., 2008). In this work, the commercial DEM software EDEM™ (DEM Solutions Ltd., Edinburgh, Scotland) with the Hertz–Mindlin (no slip) contact model is used. The modeled system consists of a lab-scale Vector LDCS (Marion, IA) 1.5 L film coating pan with diameter D = 29.2 cm rotating at speed ω as shown in Fig. 1. The pan internals include four custom-manufactured baffles positioned in an alternating configuration that traverse the length of the pan and eight small, anti-slip bars on each of the conical ends. The details of the computational system have been selected to match those from the experiments as closely as possible.

Two different sets of simulations were conducted in this work. In the first set, standard round concave (SRC) tablet shapes were modeled to compare with experimental data for validation purposes. These tablets were defined to have the same dimensions and mass as those used in the experimental system described in Section 2. In the second set of simulations, five different non-spherical tablet shapes and a sphere for comparison were modeled to determine the effect of tablet shape on coating uniformity. Fig. 2 shows both a sketch of the tablet shape and the "glued-sphere" representation from the DEM software for each of the tablet shapes. The tablet shapes included almond, bullet, half moon, shield, and SRC. In this study, the tablet shapes are quantified by two methods: sphericity and a mean aspect ratio. The sphericity, ψ, is defined as the ratio of the surface area of a sphere, A_S, with the same volume as the tablet, V_T, to the tablet's actual surface area, A_T, and is given by (Wadell, 1935):

$$\psi \equiv \frac{A_S}{A_T} = \frac{\pi^{1/3}(6V_T)^{2/3}}{A_T}. \quad (2)$$

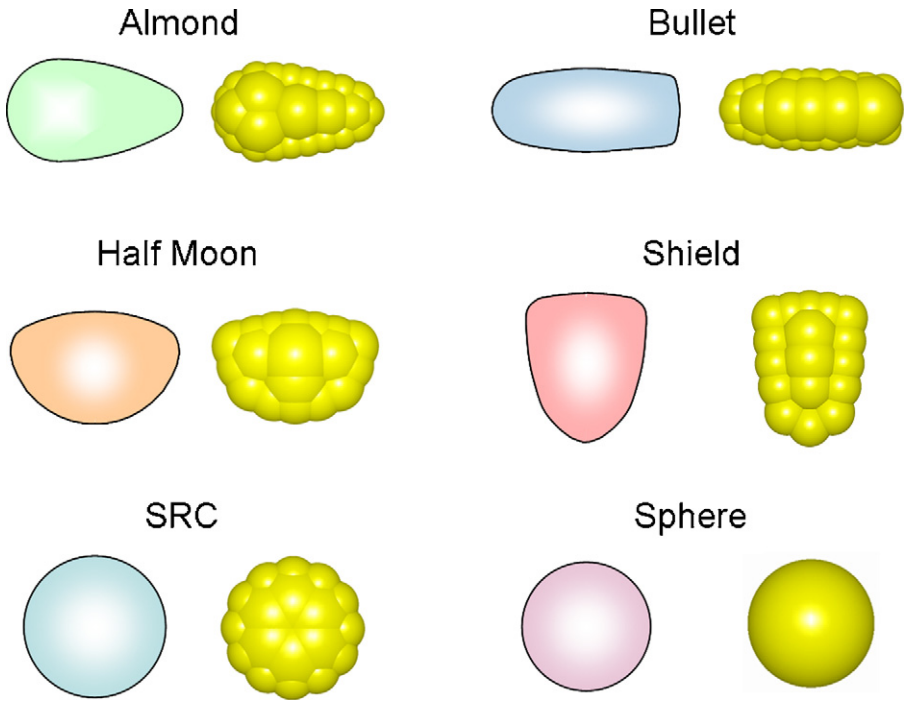

Fig. 2. The five tablet shapes investigated in the present work include (a) almond, (b) bullet, (c) half moon, (d) shield, and (e) SRC. A (f) sphere is included as a comparator. For each shape, a sketch and the glued-sphere representation in the DEM model are shown on the left and right sides, respectively.

The second method, a mean aspect ratio, A, is given by:

$$A = \frac{(L+W)}{2T} \tag{3}$$

where L, W, and T are the tablet length, width, and thickness, respectively. The mass, dimensions, and shape quantifications for each tablet shape are given in Table 1.

The number of constituent spheres used to form each tablet shape using the "glued-sphere" approach has been selected to be approximately the same for each shape. It is desired to use a sufficient number of spheres to capture the primary features of the tablet shape. On the other hand, large numbers of constituent spheres per tablet can dramatically lengthen the required computational time (Song et al., 2006). Additionally, tablet contacts that involve multiple constituent spheres may be prone to inaccuracies such as over-damping (Kodam et al., 2009; Kruggel-Emden et al., 2008). Thus, it is desired to use an intermediate number of spheres that accurately model the primary shape features without incurring the computational issues with a very large numbers of spheres. The size and position of the constituent spheres were selected by visual inspection to represent the tablet shape. However, computational algorithms to determine the optimal number, size, and position of such spheres is a matter of recent research (Ferellec and McDowell, 2008; Price et al., 2008) and could improve the tablet shape building process in the future.

The baseline process parameters and the range of values examined are shown in Table 2 for both the experimental comparison simulations and the DEM parametric studies. The process parameters for the experimental comparison simulations were selected to be equivalent to the conditions of the experimental trials. For the parametric simulations, the pan speed and load were varied in a range typical of experimental trials in a small-scale pan. Also shown in Table 2 are the material properties and interaction parameters, which were the same for both the experimental comparison and parametric simulations. The material properties of the tablets and coating pan were selected to be representative of a placebo formulation and stainless steel respectively, however, the values of the shear modulus have been reduced somewhat to reduce the computational time required. This reduction did not significantly impact the results; simulations conducted with shear moduli increased by a factor of 100 yielded mean residence and circulation times that varied by less than 1.5%. The contact parameters were based on the default values in EDEM^{TM} with the exception of rolling friction, μ_R. For the non-spherical tablets, $\mu_R = 0.0$ while for any contact

Table 1
Mass, dimensions, and shape quantifications for the tablets used in the experimental confirmation and parametric study.

Shape	Mass, m (mg)	Length, L, or diameter, D (mm)	Width, W (mm)	Thickness, T (mm)	Sphericity, ψ (–)	Mean aspect ratio, A (–)
Experimental validation						
SRC	800	11.9	–	8.3	–	–
DEM parametric study						
Almond	1300	20.6	12.1	7.4	0.840	2.22
Bullet	1300	22.4	9.8	8.0	0.872	2.01
Half moon	1300	17.8	12.6	8.8	0.893	1.76
Shield	1300	17.6	13.3	7.0	0.810	2.21
SRC	1300	12.7	–	8.9	0.953	1.42
Sphere	1300	11.9	–	–	1.00	1.00

Table 2
Baseline process parameters, material properties, and contact parameters and the range of values examined.

Parameter	Experimental comparison	DEM parametric study	
	Value	Baseline value	Range
Pan speed, RPM	22	22	(16, 28)
Pan loading, kg	0.7 and 1.0	1.5	(1.0, 2.0)
Number of tablets	~875 and 1250	~1168	(778, 1539)
Shear modulus, MPa			
Tablets	1.0	1.0	–
Steel	3.0	3.0	–
Poisson's ratio			
Tablets	0.25	0.25	–
Steel	0.30	0.30	–
Density, kg/m^3			
Tablets	1500	1500	–
Steel	7500	7500	–
Coefficient of friction, μ			
Tablet–tablet	0.5	0.5	–
Tablet–steel	0.5	0.5	–
Coefficient of restitution, e			
Tablet–tablet	0.5	0.5	–
Tablet–steel	0.5	0.5	–
Coefficient of rolling resistance,[a] μ_R			
Tablet–tablet	0.0	0.0	–
Tablet–steel	0.0	0.0	–

[a] $\mu_R = 0.0$ for all interacting pairs except those involving spheres, where $\mu_R = 0.10$.

involving a sphere, $\mu_R = 0.10$. In this work, rolling friction is included only for the spherical shape to reduce the unrealistically large rotational speeds exhibited by spherical particles (see e.g. Cleary (2009)). In contrast, by virtue of their non-spherical shape, the other tablet shapes maintain more realistic rotation speeds. Thus, the rolling friction model is not included for these shapes. The results for the spherical shape are somewhat sensitive to the value of μ_R as shown in Appendix A.

The tablet mixing dynamics were modeled for 60 s using an integration time step of 60 μs. The spray was not modeled directly, but the residence time of a tablet in a hypothetical spray zone was assumed to be proportional to the increase in film coat mass. An implicit assumption here is that the spray flux is constant, homogeneous, and uniformly distributed throughout the spray zone. This assumption is not expected to dramatically affect the results; Pandey et al. (2006a) used a Monte Carlo approach that predicted a small improvement in the coating uniformity for a uniform spray flux over what the authors called a non-uniform flux. Further, the effects of atomizing air, spray rate, drying air, droplet impact and spreading, and any effects of the liquid on tablet–tablet interactions were not considered here but have been previously discussed elsewhere (Bolleddula et al., 2010; Porter et al., 1997; Rege et al., 2002; Skultety et al., 1988; Song and Turton, 2007; Tobiska and Kleinebudde, 2003b).

To predict the coating uniformity for a given set of conditions, the tablets located within the spray zone and on the free surface of the tablet bed must be identified at a given time. Any tablet meeting these conditions is assumed to receiving coating. The size and position of the spray zone were selected to match the experimental field of view of the machine vision system: a rectangular region 7.0 cm by 15.2 cm, with the long side aligned parallel to the axis of the drum as shown in Fig. 3. To determine which tablets were on the top surface, the rectangular spray zone was subdivided with a 2-D grid of rectangular bins. The bins were on the order of the tablet dimension with a targeted side length, b, given by

$$b = 1.5\sqrt[3]{LWT} \tag{4}$$

where L, W, and T are the tablet length, width, and thickness, respectively. However, this value was adjusted such that the 7.0 cm by 15.2 cm spray zone was divided by an integer number of bins in

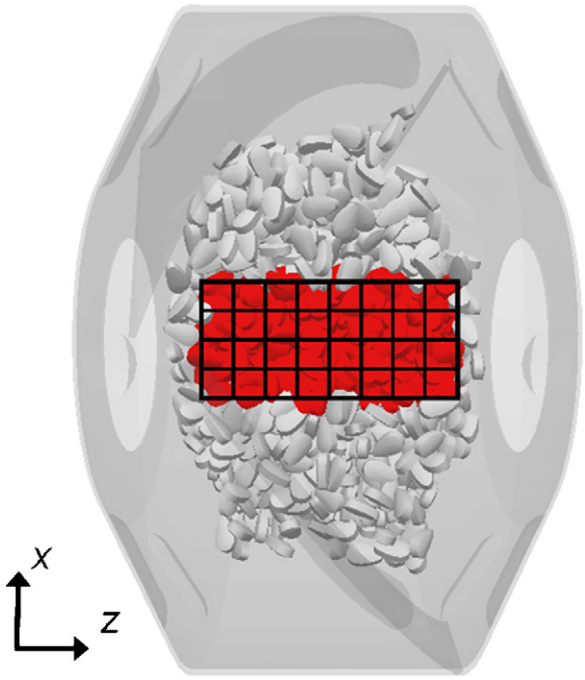

Fig. 3. The top view of the rectangular spray zone divided into a 2-D grid of 4 by 8 bins.

both dimensions. For the experimental validation study, the spray zone was divided in to a 2-D grid consisting of 4 by 10 bins while for the parametric study, the spray zone was divided in to a 2-D grid consisting of 4 by 8 bins due to the larger tablet size. This 4 by 8 grid of bins is depicted in Fig. 3. For each bin, the uppermost tablet was selected as being on the top surface of the bed. After the tablets on the top surface have been identified, the inter- and intra-tablet coating variability statistics can be calculated. The sensitivity to the bin size was examined in the experimental validation study. The sensitivity study showed that for bin sizes considerably smaller than b, tablets within the bulk were erroneously identified as being on the free surface. For bin sizes considerably larger than b, tablets located on the free surface were frequently not identified.

The inter-tablet coating variability is a function of the number of passes through the spray zone, the length of time a tablet spends in the spray zone, and the variability in these measurements between tablets. These quantities are determined by compiling the appearance statistics of each tablet during the course of the simulation. In increments of 20 ms, the tablets that are within the spray zone and are positioned on the top surface are determined as described above. For each consecutive time increment that a given tablet remains within the spray zone and on the top surface, the time in the spray zone is incremented by an additional 20 ms. If the tablet should drop below the top surface and reappear within the spray zone within a threshold time of $t_c = 100$ ms, only one pass through the spray zone is counted, and those time increments spent below the top surface are not added to the time in the spray zone. The threshold time of $t_c = 100$ ms was selected to match the experimental procedure. Further, a sensitivity analysis has shown that the results vary considerably for smaller t_c times, however only vary by <5% for $t_c = 200$ ms. Other recent work has used threshold values of 500 ms (Sandadi et al., 2004) however, in this case, a larger diameter pan ($D = 57.5$ cm) was used. Once all the appearance data is collected, the distributions of the residence time in the spray zone per pass and the circulation time between passes are determined. The median values and the range between the 10th and 90th percentiles are reported in Section 5 to quantify inter-tablet coating variability.

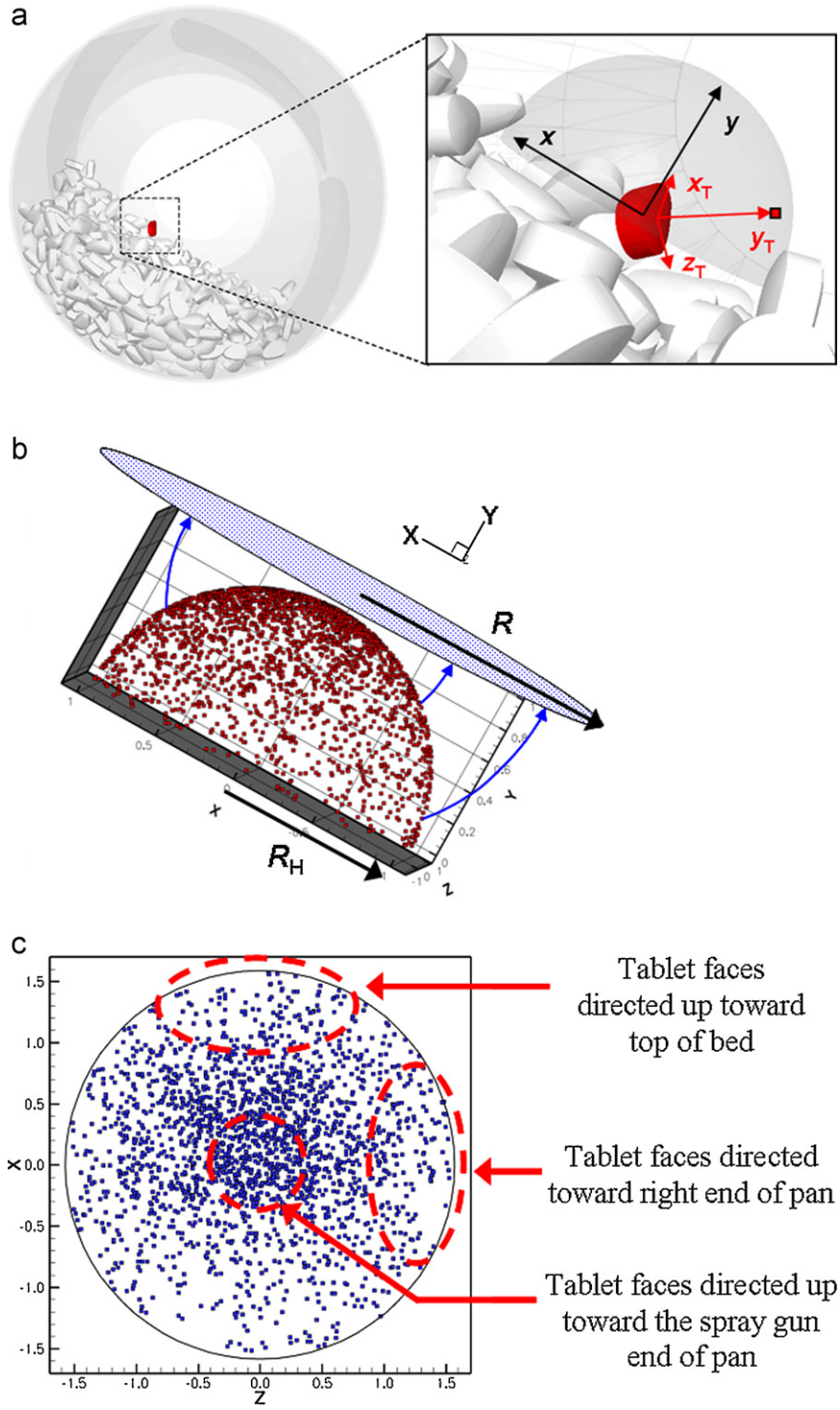

Fig. 4. Images depicting the determination and analysis of tablet orientations in the spray zone (spray zone not shown for clarity). (a) For a given tablet, the unit vector describing the direction of the tablet face, y_T, is determined. Repeating this process for all tablets in the spray zone produces data within a hemispherical domain (b) which is then transformed to a 2-D plot using an exponential mapping. (c) The 2-D data shows the distribution of directions of the tablet faces, and the position of each data point can be related to the tablet orientation in the coating pan.

The intra-tablet coating variability is a function of the orientation of tablets as they pass through the spray zone. These data are provided by the EDEM^{TM} software as a matrix of direction cosines. While these contain the direction data for each of the three principal axes of the tablet, the current analysis focuses only on the direction of the tablet face, $\boldsymbol{y}_T$, as shown in Fig. 4(a). This is sufficient to characterize the intra-tablet coating variability since previous experimental work has shown that this type of variability is generally observed as differences in coating thickness between the face and the tablet band (either the side or end) (Ho et al., 2007; Perez-Ramos et al., 2005; Wilson and Crossman, 1997). For each tablet in the spray zone, the direction of the unit vector normal to the tablet face $\boldsymbol{y}_T$ that is pointed up toward the spray gun (as opposed to down toward the bulk of the tablet bed) is determined as shown in Fig. 4(a). This is repeated for every tablet on the surface of the bed and within the spray zone. These data, collected at a frequency of

once per second, populate a hemispherical domain of unit radius, $R_H = 1$, as depicted in Fig. 4(b). The geodesic mean, $\boldsymbol{\mu}$, of these data is then calculated (Buss and Fillmore, 2001). The standard deviation of $\mathbf{y}_T$ directions for the given shape j, σ_j, then is calculated using the mean geodesic distance, $d(\boldsymbol{\mu}, \mathbf{y}_{T,i})$, from each of these points to the previously calculated mean value, $\boldsymbol{\mu}$ (Fletcher et al., 2004):

$$\sigma_j = \sqrt{\frac{1}{N}\sum_{i=1}^{N} d(\boldsymbol{\mu}, \mathbf{y}_{T,i})^2} \quad (5)$$

where N is the total number of tablet orientation data points analyzed. To more clearly present the 3-D, hemispherical distribution of tablet face directions depicted in Fig. 4(b), an exponential mapping (Buss and Fillmore, 2001) is used here to plot the data in a 2-D format. Following the exponential mapping, the radius of this now circular domain $R = \pi/2$. This mapping maintains the relative direction and geodesic distance of the original hemispherical data, but is more easily visualized, as shown in Fig. 4(c). It should also be noted that the position of the data points in Fig. 4(c) can be related back to the tablet orientation in the film coating pan. For instance, points near the top (right side) of Fig. 4(c) indicate that the tablet is tilted so the face is pointed toward the top of the cascading bed (right side of pan).

An Orientation Index (OI) is introduced to describe the variability of tablet orientation in the spray zone, and hence, the intra-tablet coating variability, in a more quantitative manner. The OI is defined as:

$$OI = \sigma_{\text{Ideal}} - \sigma_{\text{Tablet}} \quad (6)$$

where, for the ideal case of uniformly distributed points, $\sigma_{\text{Ideal}} = (2R/3) = (\pi/3)$. Thus, tablet shapes with a strongly preferred orientation in the spray zone will have a small σ_{Tablet} value and a large OI. Such a shape will have significant intra-tablet coating variability (significantly greater coating thickness on the tablet face compared to the tablet band). Tablet shapes that do not have a preferred orientation in the spray zone (i.e. close to spherical shape), will not exhibit a preferred orientation in the spray zone and, consequently, $\sigma_{\text{Tablet}} \approx \sigma_{\text{Ideal}}$ and OI is small. Such a shape will have minimal intra-tablet coating variability (relatively uniform coating thickness on all sides of the tablet).

4. Experimental confirmation of model

Experimental trials were conducted to compare data with the DEM model predictions. All parameters such as the pan size and geometry, pan load, pan speed, as well as the size, shape, and number of tablets were selected to be as similar as possible. Three key statistics characterizing tablet appearances in the spray zone, and thus, tablet mixing, were calculated for both the experiments and simulations. These are summarized in Table 3 for both a 1.0 kg and 0.7 kg pan load. In each case, the agreement between the experimental data and DEM predictions is within ±5%. The distributions of the mean residence time per pass and circulation time between passes are plotted in Fig. 5 for (a) 1.0 kg pan loading and (b) 0.7 kg pan loading. In each case, reasonably good agreement is observed between the DEM predictions and the experimental data. The DEM model predicts a somewhat larger peak in the circulation time distribution, however, the model still captures the considerable frequency of long circulation times observed experimentally. This is

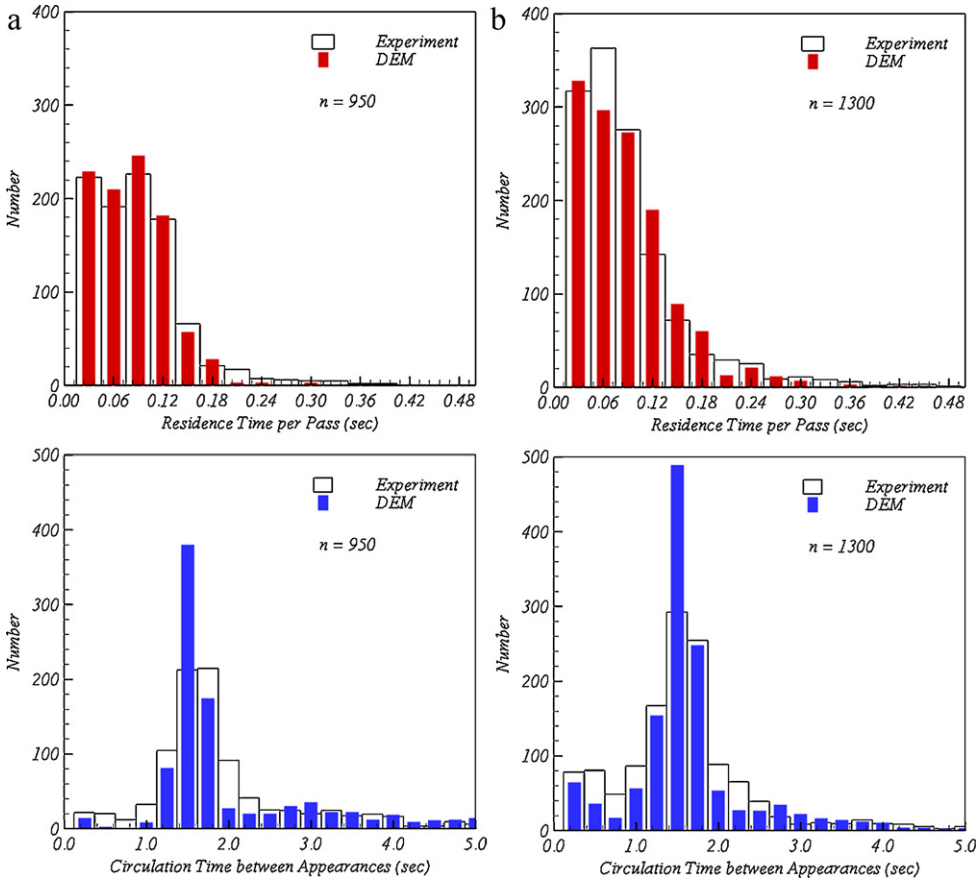

Fig. 5. Distribution of residence time per pass and circulation time between appearances for (a) 1.0 kg pan loading and (b) 0.7 kg pan loading.

Table 3
Comparison of the experimental measurements and DEM model predictions for three key tablet appearance statistics for two different pan loads.

	Experiment	DEM model	Percent difference
1.0 kg pan loading			
Appearance frequency (1/min)	30.6	30.0	−2.0%
Mean circulation time between appearances (s)	1.92	1.92	0.2%
Mean residence time per pass (s)	0.082	0.080	−2.9%
0.7 kg pan loading			
Appearance frequency (1/min)	39.5	37.4	−5.3%
Mean circulation time between appearances (s)	1.51	1.52	0.7%
Mean residence time per pass (s)	0.090	0.087	−3.6%

important because it is this variability that significantly impacts inter-tablet coating variability.

5. Results and discussion

The results are presented in two parts: inter-tablet coating uniformity is first discussed followed by intra-tablet coating uniformity. In each part, the effects of tablet shape, pan loading, and pan speed on coating uniformity are examined.

5.1. Inter-tablet coating uniformity

Achieving good inter-tablet coating uniformity requires that both the residence time in the spray zone and the circulation time between appearances are narrowly distributed. Should either of these distributions be overly broad, significant variability in film coating thickness can result. In the following figures, the median values of the tablet residence time in the spray zone per pass and the circulation time between consecutive appearances are reported. Scatter bars denoting the 10th and 90th percentiles provide an indication of the variability associated with the reported values. Note that the time resolution of the simulation data is 0.02 s, so data on small time scales (i.e. residence time data) appears in increments of 0.02 s.

Fig. 6(a) and (b) shows the distributions of residence time and circulation time for the five different tablet shapes and a sphere for comparison for a pan loading of 1.5 kg and pan speed of 22 RPM. The residences times are similar for each shape. The median values vary between 0.06 s and 0.08 s and the ranges, given by the difference between the 10th and 90th percentiles, are equivalent. Further, the circulation time distributions are also similar for all of the non-spherical tablet shapes tested here. The distribution for the spherical shape is slightly narrower, but is dependent on the value of the rolling friction (Appendix A). For each shape, the circulation times are positively skewed indicating that for a small portion of the tablet appearances, there is a long time (~4–5 s) between consecutive appearances in the spray zone as compared to typical circulation times (~1.5 s) at these conditions. These long circulation times are often due to tablets bypassing the spray either just underneath the free surface or around either end near the conical ends of the pan as shown by the simulation videos. Based on the residence time and circulation time results in Fig. 6, tablet shape is not expected to have a significant effect on inter-tablet coating uniformity. This result – for five different tablet shapes – is in agreement with the experimental work of Pandey et al. (2005) that found little difference in residence time and circulation time between one tablet shape (SRC) and spherical particles. However, as shown in Appendix A, significant differences between the non-spherical tablets and the spherical shape can be observed depending on the value of the rolling friction coefficient for the spheres.

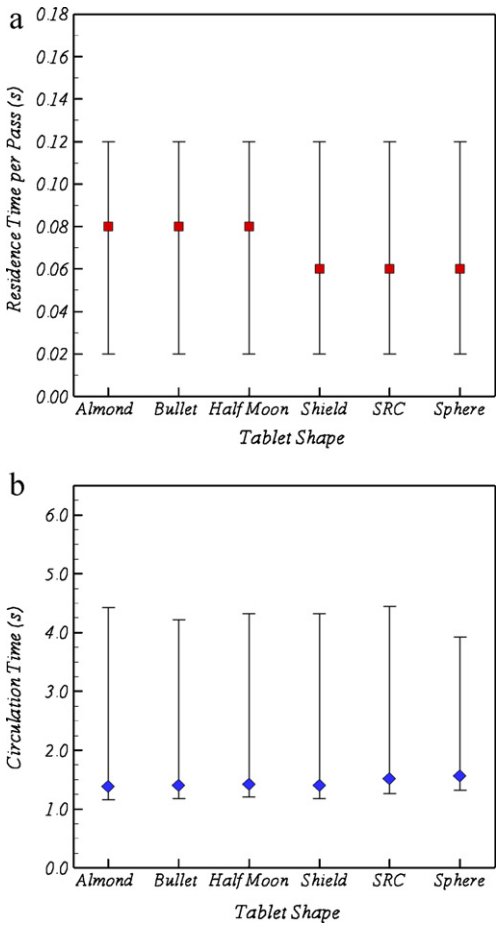

Fig. 6. The effect of tablet shape on tablet appearance statistics (a) residence time per pass and (b) circulation time for fixed pan speed of 22 RPM and pan loading of 1.5 kg.

The effect of pan loading on residence time and circulation time is shown in Fig. 7(a) and (b) for the almond tablet shape and a pan speed of 22 RPM. Both the residence time median and range decrease with pan load. Leaver et al. (1985) suggested this was due to a steeper angle of repose of the bed for increasing loads, resulting in tablets moving down the free surface with greater velocity and, consequently, shorter residence times. The trends reported here are in agreement with several previous reports for spheres and/or SRC tablets (Leaver et al., 1985; Pandey et al., 2005; Sandadi et al., 2004; Yamane et al., 1995), however Kalbag et al. (2008) reported decreasing values for large pan speeds, but the presence of a maximum for smaller pan speed due to slumping behavior at low loadings. The circulation time results show that both the median values and ranges increase with increasing pan load. Observation of increasing mean circulation times has been reported previously for spheres and/or SRC tablets (Leaver et al., 1985; Pandey et al., 2005; Sandadi et al., 2004; Yamane et al., 1995) but the present work also shows that the range of circulation times increases dramatically with pan load. The increase in the median circulation time is due to a somewhat greater distance required to complete one cycle of travel around the pan. The increase in the range is due to a greater probability of the tablets bypassing the spray zone – generally by passing under the free surface – for the larger bed depths present for larger pan loads. Based on the results in Fig. 7, the inter-tablet coating variability will tend to increase for larger pan loads. While the variability in residence time per pass decreases with increasing pan load, the variability in circulation time significantly increases with pan load, more than offsetting the variability in residence time.

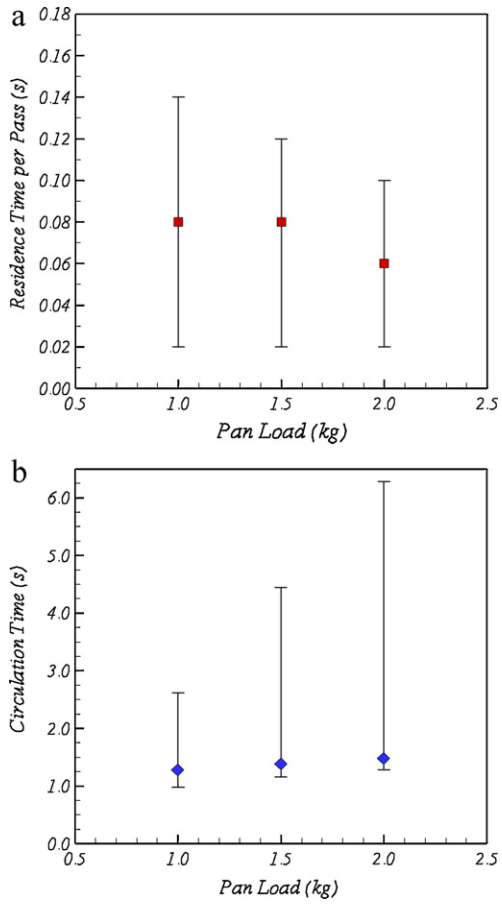

Fig. 7. The effect of pan loading on tablet appearance statistics (a) residence time per pass and (b) circulation time for fixed pan speed of 22 RPM and the almond tablet shape.

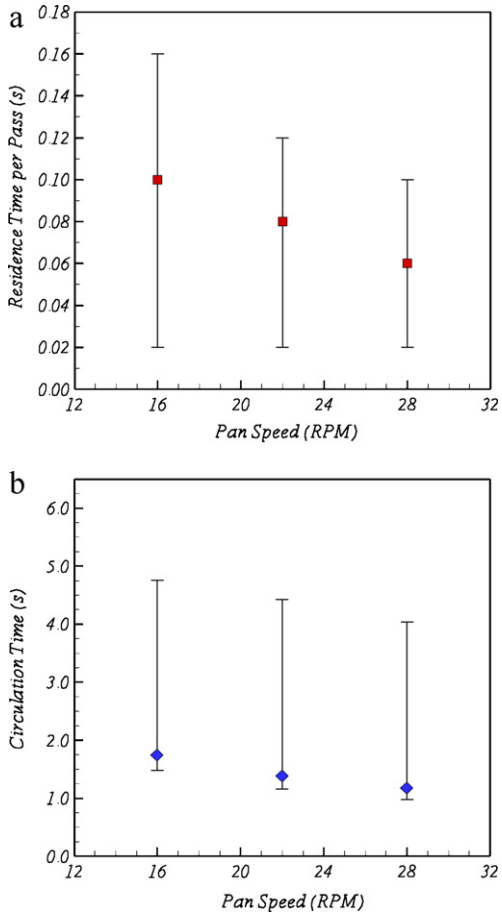

Fig. 8. The effect of pan speed on tablet appearance statistics (a) residence time per pass and (b) circulation time for fixed pan loading of 1.5 kg and the almond tablet shape.

The effect of pan speed on residence time and circulation time is shown in Fig. 8(a) and (b) for the almond tablet shape and a pan load of 1.5 kg. The residence time median and range decrease with increasing pan speed. For faster pan speeds, the tablet velocities on the free surface are also faster in agreement with Alexander et al. (2002), resulting in shorter residence times in the spray zone. Similar observations have been made in several previous reports for spheres and/or SRC shaped tablets regarding the mean values (Leaver et al., 1985; Pandey et al., 2005; Sandadi et al., 2004) and ranges (Leaver et al., 1985; Yamane et al., 1995). The median circulation time decreases with pan speed but the range is approximately constant over the pan speeds tested here. The circulation times tend to decrease for faster pan speeds because the tablets are moving with greater speeds and therefore complete a cycle around the pan in a shorter amount of time. The distribution of circulation times remains relatively constant because there is the same probability of tablet bypassing the spray zone either around the end or just underneath the free surface. Previous researchers have also reported a decrease in mean circulation times for spheres and/or SRC shaped tablets (Leaver et al., 1985; Pandey et al., 2005; Sandadi et al., 2004; Yamane et al., 1995) and relatively constant ranges of circulation times (Pandey et al., 2005) with increasing pan speeds. The current work extends these results for the tablet shapes examined here. Based on the results in Fig. 8, the inter-tablet coating variability will tend to decrease for faster pan speeds. The variability in residence time decreases with speed while the variability in circulation time is approximately constant. In addition, for a fixed period of time, there will be a greater number of coating events per tablet for faster pan speeds. This will also contribute to improved inter-tablet coating uniformity (Eq. (1)).

5.2. Intra-tablet coating uniformity

Achieving good intra-tablet coating uniformity requires that the tablet orientations in the spray zone are relatively uniformly distributed such that there is not a preferred orientation as the tablets pass through the spray zone. Fig. 9 shows plots of tablet orientations (specifically, the direction normal to the tablet face) in the spray zone for each of the five tablet shapes and the spherical shape for comparison. Each data point represents the direction of a tablet face while in the spray zone. For the almond and shield tablet shapes, there is a large concentration of points near the center of the plot indicating a preferred orientation in which the tablet faces are generally facing up toward the spray gun. A slight bias toward positive x values indicates that the faces tend to be slightly tilted toward the top of the cascading bed. In each case, there are a limited number of points around the periphery of the plot indicating that there are fewer appearances in which the tablet bands (edges and ends of tablets) are coated. Therefore, significant intra-tablet coating variability is expected for the almond and shield shapes. The bullet and half moon shapes also exhibit large concentrations of points near the center of the plots, however, these concentrations are less extreme than those for the almond and shield shapes. As a result, the bullet and half moon have a somewhat less strongly preferred orientation as compared to the almond and shield. Finally, the SRC shape has orientations that are fairly well distributed, and

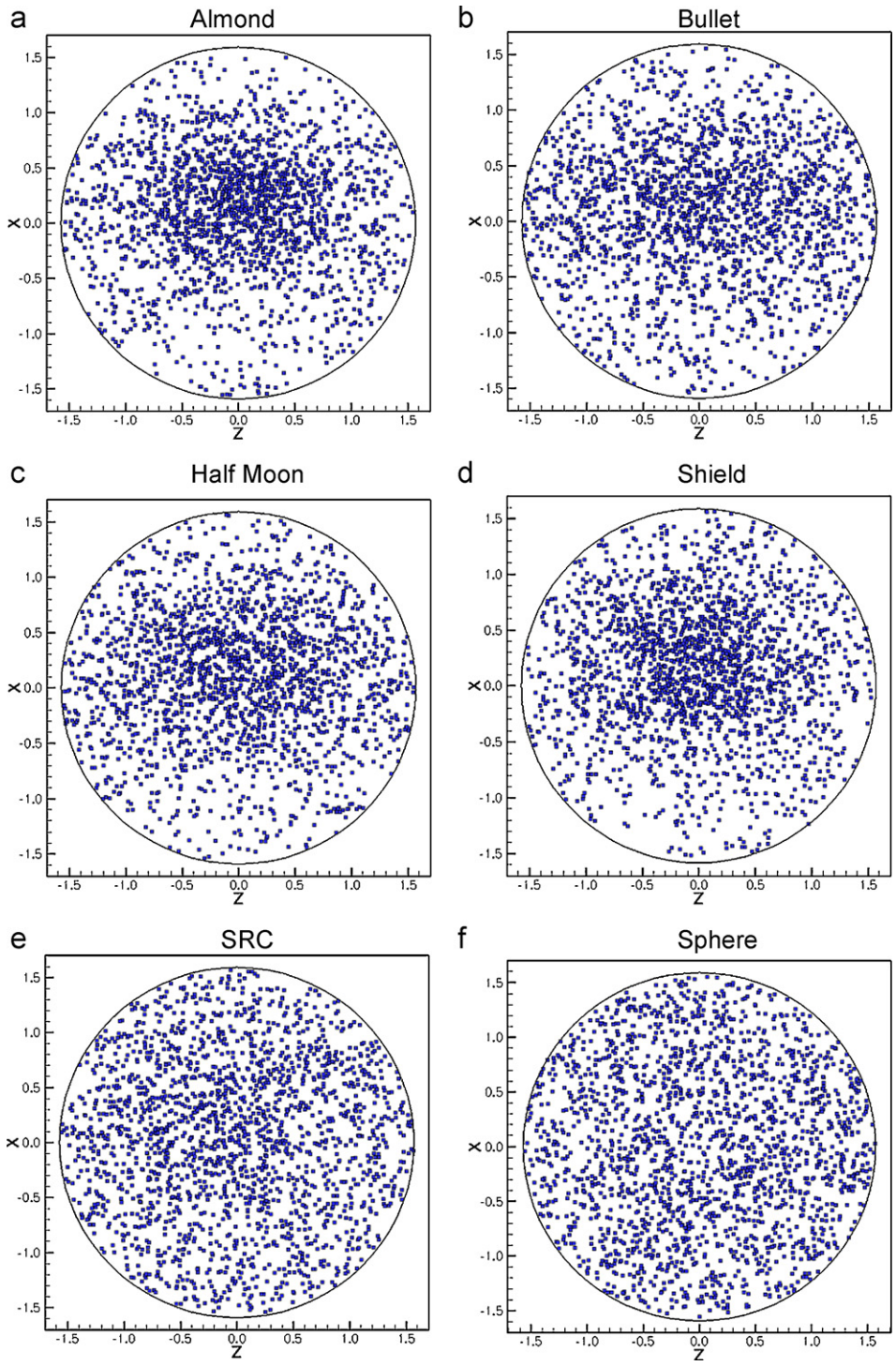

Fig. 9. Scatter plots showing the orientation of each tablet passing through the spray zone region over the course of the simulation time for (a) almond, (b) bullet, (c) half moon, (d) shield, and (e) SRC tablet shapes with (f) a sphere for comparison.

therefore good intra-tablet coating uniformity is predicted. The data for the sphere is the most uniformly distributed as expected since the spherical shape is isotropic and therefore does not have any preferred orientation.

A more quantitative analysis of the data shown in Fig. 9 is given by the Orientation Index (*OI*) calculated using Eqs. (5) and (6) and reported in Table 4. These *OI* values correlate with the qualitative assessment described above where larger *OI* values indicate a more strongly preferred orientation in the spray zone and a more significant concentration of points in the corresponding plot in Fig. 9.

Spherical shapes represent the limiting case where no preferred orientation is observed and *OI* = 0.0. Thus, it stands to reason that shapes with increasing departure from spherical may exhibit increasingly intense preferred orientations. In Fig. 10(a), the orientation indices from Table 4 are plotted as a function of the inverse of the respective tablet sphericities ψ. A reasonably good correlation is shown for the six shapes examined here. In practice, however, during the selection of the shape and size of a pharmaceutical tablet, the surface area and volume required to calculate ψ may not be readily known. In such cases, it is desirable to use a proxy for tablet

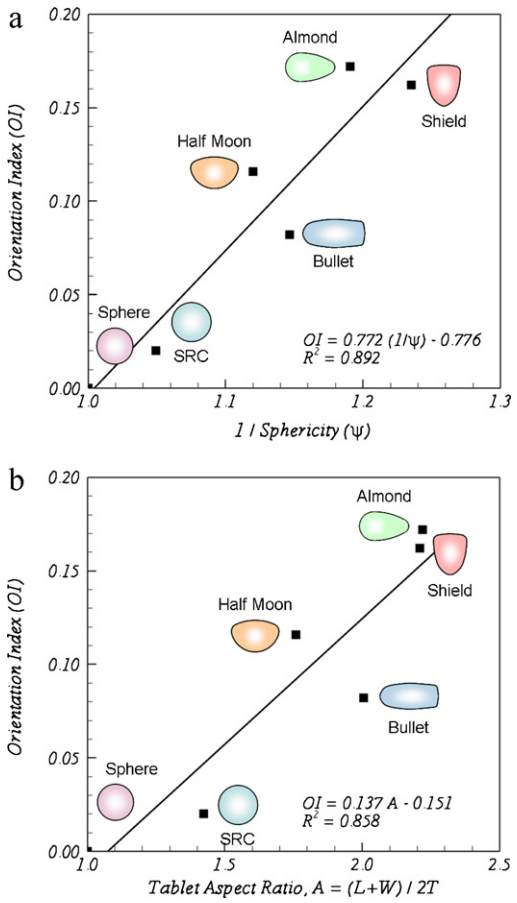

Fig. 10. Tablet orientation indices predicted from DEM model plotted as a function of (a) the tablet sphericity and (b) a mean tablet aspect ratio *A*.

sphericity. In Fig. 10(b), the orientation indices are plotted as a function of a mean tablet aspect ratio, *A*. Again, a reasonably good correlation is shown for the six shapes examined here.

These simple measures of tablet shape – sphericity and aspect ratio – both describe the propensity of a given tablet shape to tumble, or rotate end over end. The tablet shapes with sphericities or aspect ratios close to unity (e.g. spheres, SRC) will readily tumble through the spray zone and have a low intra-tablet coating variability. Those tablets shapes with relatively small sphericities or large aspect ratios (e.g. almond, shield) will only tumble a limited amount. The results in Fig. 9(a) and (d) show that these shapes will likely slide through the spray zone with a face directed up toward the spray zone which will result in large intra-tablet coating variability.

Wilson and Crossman (1997) reported experimental data for intra-tablet coating uniformity for capsule, large oval, small oval, and SRC tablet shapes. Based on the tablet dimensions in that report, the intra-tablet coating uniformity tends to improve with decreasing average aspect ratio, *A*, similar to the present work. However, the correlation of the Wilson and Crossman (1997) data improved when using the simpler aspect ratio *L*/*T*. Based on the relatively limited number of tablet shapes examined here and in Wilson and Crossman (1997), it is unclear which geometric descriptor is best for a wide variety of tablet shapes, but intra-tablet uniformity data all tend show at least a fair correlation with ψ, *A*, and *L*/*T*.

Table 4
Orientation indices for the six shapes.

Shape	Orientation Index (*OI*)
Almond	0.172
Bullet	0.082
Half moon	0.116
Shield	0.162
SRC	0.020
Sphere	0.000

Table 5
Orientation indices for the almond tablet shape and the given pan speed and loading.

Pan speed	Pan load	Orientation Index (*OI*)
22 RPM	1.0 kg	0.158
22 RPM	1.5 kg	0.172
22 RPM	2.0 kg	0.179
16 RPM	1.5 kg	0.173
22 RPM	1.5 kg	0.172
28 RPM	1.5 kg	0.140

Since the almond shape exhibited the most strongly preferred orientation of the six shapes investigated, additional simulations focusing solely on the almond shape are conducted to determine the effects of pan speed and pan loading on intra-tablet uniformity. The effect of pan loading on the distribution of almond tablet orientations is observed to be minimal; the plots of tablet orientations for varying speed all appear similar to that in Fig. 9(a). The *OI* for each of these cases is summarized in Table 5. The *OI* does show some improvement for reduced pan loadings, but the extent is fairly small as compared to the range of *OI* values for other shapes (Table 4 or Fig. 10). The reason for the reduced *OI* for lower pan loads is not clear, but the simulation videos do show that the flow for the 1 kg pan load appears to be more chaotic while that for the 2 kg pan load appears to be more uniform and orderly. In addition, the mean angular velocity of tablets in the spray zone is greater for the 1 kg pan load. As such, the tablets are more likely to exhibit tumbling or rotating motion through the spray zone.

The effect of pan rotation speed on the distribution of almond tablet orientations is also relatively small. The *OI* for each of these cases is summarized in Table 5. This shows that there is little difference between 16 and 22 RPM, but the *OI* does improve for the fastest speed 28 RPM. This is potentially due to a transition from the cascading flow regime into the cataracting flow regime (Mellmann, 2001) where the tablets have a greater kinetic energy and have a greater probability to briefly become airborne and rotate away from the preferred orientation (tablet face directed up toward spray gun). For a rotating cylindrical drum without mixing elements or baffles, Mellmann (2001) specifies that the transition point between the two regimes is where the Froude number Fr = 0.1. For the present system, 22 RPM → Fr = 0.079 (cascading regime) and 28 RPM → Fr = 0.123 (cataracting regime).

6. Conclusions

A DEM model for tablet film coating is developed and confirmed with experimental data in a film coating pan of the same dimensions using a machine vision system. The model is then used to predict the relative impact of a variety of novel pharmaceutical tablet shapes and process parameters on both inter- and intra-tablet film coating uniformity. The results show that tablet shape significantly affects the intra-tablet coating uniformity. This effect is quantified and is shown to correlate fairly well with the mean tablet aspect ratio. In contrast, the tablet shape appears to have little effect on inter-tablet coating uniformity. The effects of varying pan loading and pan speed were examined for the almond tablet shape. Slight improvements in the intra-tablet coating uniformity were observed for smaller pan loads or faster pan speeds; however, the magnitude of these improvements is generally smaller than what can be obtained by changing the tablet shape. The pan loading and pan speed had a more pronounced effect on the

inter-tablet coating uniformity where faster pan speeds and smaller pan loads tend to improve uniformity.

This work shows that tablet shape is the key parameter affecting intra-tablet coating uniformity. While the pan speed and pan loading have a small effect, there is little one can do to improve intra-tablet coating uniformity for a given tablet shape. Using this approach, preferred tablet shapes that will minimize intra-tablet coating variability can be identified prior to manufacture of the compression tooling and tablets. Inter-tablet coating variability can be reduced through optimization of the pan speed and pan loading subject to the competing factors such as reduced throughput for small batch sizes and possible tablet attrition at large pan speeds. Improved coating uniformity will help to increase process efficiency in the case of aesthetic coats, improve content uniformity for active coats, and reduce the variability of drug release profiles for controlled release coats.

Acknowledgements

Insightful discussions with Carl Wassgren, Ben Freireich, and Pfizer colleagues Mary am Ende, Al Berchielli, Rahul Bharadwajh, Bruno Hancock, and Barb Johnson are gratefully acknowledged. Bend Research Inc. and, in particular Mark Chidlaw, are acknowledged for providing the experimental data and procedural details.

Appendix A.

The effects of rolling friction on the residence time and circulation time for the spherical tablet shape are shown in Fig. A.1. Both

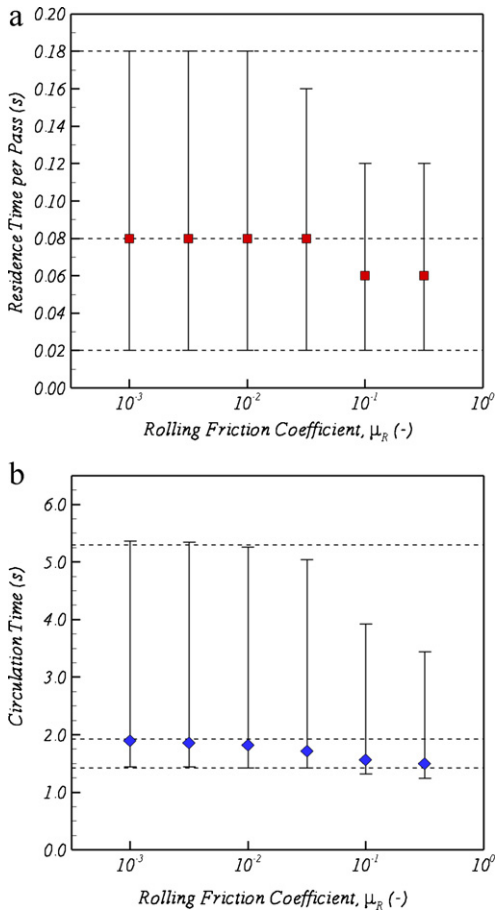

Fig. A.1. The effect of rolling friction on tablet appearance statistics (a) residence time per pass and (b) circulation time for the spherical shape, a fixed pan speed of 22 RPM, and pan loading of 1.5 kg. The dashed lines indicate the median, 10th and 90th percentiles for the case of $\mu_R = 0$.

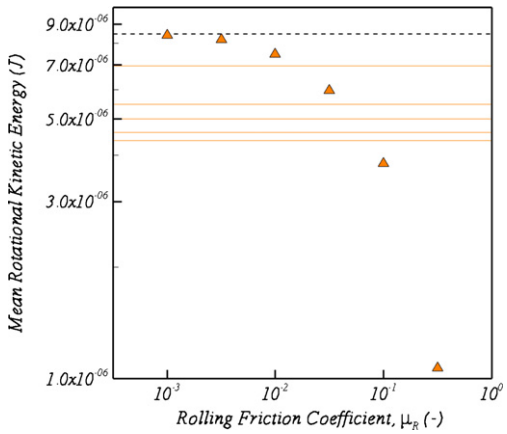

Fig. A.2. The mean rotational kinetic energy of all tablets as a function of rolling friction. The solid horizontal lines indicate the values for each of the non-spherical tablets. The dashed horizontal line indicates the value for spheres with $\mu_R = 0$.

distributions show little change for $0 \le \mu_R \le 0.01$, but for larger μ_R however, the distributions narrow indicating more uniform circulation and residence times in the spray zone. This is a result of an increased dynamic angle of repose for larger μ_R values, consistent with the observations of Zhou et al. (2002). The increased repose angles result in faster surface velocities and, consequently, shorter residence and circulation times. The distribution data in Fig. 6(a) and (b) show little or no difference between the non-spherical shapes and the spheres with $\mu_R = 0.10$. However, there would be significant differences – namely, a much wider distribution – had the non-spherical shapes been compared to spheres with $\mu_R = 0$. It should also be noted that there is no observed effect of rolling friction on the *OI* or the intra-tablet coating uniformity as this is a function of tablet orientation and not rotation speed.

Spherical particles are known to have excessively large rotation speeds in comparison with non-spherical shapes (Cleary, 2009). In many DEM models consisting of spherical particles, rolling friction is included to reduce these rotation speeds to levels exhibited by non-spherical particles. For increasing μ_R, the particle rotation speed and, consequently the mean rotational kinetic energy, decreases as shown in Fig. A.2. For this system, values of $0.01 \le \mu_R \le 0.10$ yield mean rotational kinetic energy values similar to those for the non-spherical tablet shapes (shown with solid horizontal lines) and therefore are reasonable values to use for the purpose of reducing excessive spherical rotation speeds. Note that these μ_R values are somewhat larger than those measured for typical pharmaceutical tablets (cylindrical tablet rolling on its band) which are on the order of 0.01 (Ketterhagen et al., 2010).

References

Alexander, A., Shinbrot, T., Muzzio, F.J., 2002. Scaling surface velocities in rotating cylinders as a function of vessel radius, rotation rate, and particle size. Powder Technol. 126, 174–190.

Bolleddula, D.A., Berchielli, A., Aliseda, A., 2010. Impact of a heterogeneous liquid droplet on a dry surface: application to the pharmaceutical industry. Adv. Colloid Interface Sci. 159, 144–159.

Buss, S.R., Fillmore, J.P., 2001. Spherical averages and applications to spherical splines and interpolation. ACM Trans. Graph. 20, 95–126.

Chang, R.-K., Leonzio, M., 1995. The effect of run time on the inter-unit uniformity of aqeuous film coating applied to glass beads in a Hi-Coater. Drug Dev. Ind. Pharm. 21, 1895–1899.

Cleary, P.W., 2009. Industrial particle flow modelling using discrete element method. Eng. Comput. 26, 698–743.

Cundall, P., Strack, O.D.L., 1979. A discrete numerical model for granular assemblies. Géotechnique 29, 47–65.

Denis, C., Hemati, M., Chulia, D., Lanne, J.Y., Buisson, B., Daste, G., Elbaz, F., 2003. A model of surface renewal with application to the coating of pharmaceutical tablets in rotary drums. Powder Technol. 130, 174–180.

Džiugys, A., Peters, B., 2001. An approach to simulate the motion of spherical and non-spherical fuel particles in combustion chambers. Granul. Matter 3, 231–265.
Ferellec, J.-F., McDowell, G.R., 2008. A simple method to create complex particle shapes for DEM. Geomech. Geoeng. 3, 211–216.
Fletcher, P.T., Lu, C., Pizer, S.M., Joshi, S., 2004. Principal geodesic analysis for the study of nonlinear statistics of shape. IEEE Trans. Med. Imaging 23, 995–1005.
Freireich, B., Ketterhagen, W.R., Wassgren, C.R., 2011. Intra-tablet coating variability for common pharmaceutical tablet shapes. Chem. Eng. Sci., in press.
Freireich, B., Wassgren, C., 2010. Intra-particle coating variability: analysis and Monte-Carlo simulations. Chem. Eng. Sci. 65, 1117–1124.
Ho, L., Müller, R., Römer, M., Gordon, K.C., Heinämäki, J., Kleinebudde, P., Pepper, M., Rades, T., Shen, Y.C., Strachan, C.J., Taday, P.F., Zeitler, J.A., 2007. Analysis of sustained-release tablet film coats using terahertz pulsed imaging. J. Control. Release 119, 253–261.
Hogue, C., 1998. Shape representation and contact detection for discrete element simulations of arbitrary geometries. Eng. Comput. 15, 374–390.
Kalbag, A., Wassgren, C., 2009. Inter-tablet coating variability: tablet residence time variability. Chem. Eng. Sci. 64, 2705–2717.
Kalbag, A., Wassgren, C., Sumana Penumetcha, S., Pérez-Ramos, J.D., 2008. Inter-tablet coating variability: residence times in a horizontal pan coater. Chem. Eng. Sci. 63, 2881–2894.
Ketterhagen, W.R., am Ende, M.T., Hancock, B.C., 2009. Process modeling in the pharmaceutical industry using the discrete element method. J. Pharm. Sci. 98, 442–470.
Ketterhagen, W.R., Bharadwaj, R., Hancock, B.C., 2010. The coefficient of rolling resistance (CoRR) of some pharmaceutical tablets. Int. J. Pharm. 392, 107–110.
Kodam, M., Bharadwaj, R., Curtis, J., Hancock, B., Wassgren, C., 2009. Force model considerations for glued-sphere discrete element method simulations. Chem. Eng. Sci. 64, 3466–3475.
Kodam, M., Bharadwaj, R., Curtis, J., Hancock, B., Wassgren, C., 2010a. Cylindrical object contact detection for use in discrete element method simulations. Part I – contact detection algorithms. Chem. Eng. Sci. 65, 5852–5862.
Kodam, M., Bharadwaj, R., Curtis, J., Hancock, B., Wassgren, C., 2010b. Cylindrical object contact detection for use in discrete element method simulations. Part II – experimental validation. Chem. Eng. Sci. 65, 5863–5871.
Kruggel-Emden, H., Rickelt, S., Wirtz, S., Scherer, V., 2008. A study on the validity of the multi-sphere discrete element method. Powder Technol. 188, 153–165.
Leaver, T.M., Shannon, H.D., Rowe, R.C., 1985. A photometric analysis of tablet movement in a side-vented perforated drum (Accela-Cota). J. Pharm. Pharmacol. 37, 17–21.
Mancoff, W.O., 1998. Film coating compressed tablets in a continuous process. Pharm. Technol. Yearbook, 12–18.
Mann, U., 1983. Analysis of spouted-bed coating and granulation. 1. Batch operation. Ind. Eng. Chem. Process Des. Dev. 22, 288–292.
Mann, U., Rubinovitch, M., Crosby, E.J., 1979. Characterization and analysis of continuous recycle systems. AIChE J. 25, 873–882.
Mellmann, J., 2001. The transverse motion of solids in rotating cylinders – forms of motion and transition behavior. Powder Technol. 118, 251–270.
Mueller, R., Kleinebudde, P., 2007. Prediction of tablet veloctiy in pan coaters for scale-up. Powder Technol. 173, 51–58.
Pandey, P., Katakdaunde, M., Turton, R., 2006a. Modeling weight variability in a pan coating process using Monte Carlo simulations. AAPS PharmSciTech 7, E1–E10.
Pandey, P., Song, Y., Kayihan, F., Turton, R., 2005. Movement of different-shaped particles in a pan-coating device using novel video-imaging techniques. AAPS PharmSciTech 6, E237–E244.
Pandey, P., Song, Y., Kayihan, F., Turton, R., 2006b. Simulation of particle movement in a pan coating device using discrete element modeling and its comparison with video-imaging experiments. Powder Technol. 161, 79–88.
Perez-Ramos, J.D., Findlay, W.P., Peck, G., Morris, K.R., 2005. Quantitative analysis of film coating in a pan coater based on in-line sensor measurements. AAPS PharmSciTech 6, E127–E136.
Porter, S.C., Verseput, R.P., Cunningham, C.R., 1997. Process optimization using design of experiments. Pharm. Technol., 1–7.
Price, M., Murariu, V., Morrison, G., 2008. Sphere Clump Generation and Trajectory Comparison for Real Particles. DEM 2007, Brisbane, Austrailia.
Rege, B.D., Gawel, J., Kou, J.H., 2002. Identification of critical process variables for coating actives onto tablets via statistically designed experiments. Int. J. Pharm. 237, 87–94.
Sandadi, S., Pandey, P., Turton, R., 2004. In situ, near real-time acquisition of particle motion in rotating pan coating equipment using imaging techniques. Chem. Eng. Sci. 59, 5807–5817.
Skultety, P.F., Rivera, D., Dunleavy, J., Lin, C.T., 1988. Quantitation of the amount and uniformity of aqueous film coating applied to tablets in a 24″ Accela-Cota. Drug Dev. Ind. Pharm. 14, 617–631.
Song, Y., Turton, R., 2007. Study of the effect of liquid bridges on the dynamic behavior of two colliding tablets using DEM. Powder Technol. 178, 99–108.
Song, Y., Turton, R., Kayihan, F., 2006. Contact detection algorithms for DEM simulations of tablet-shaped particles. Powder Technol. 161, 32–40.
Tobiska, S., Kleinebudde, P., 2003a. Coating uniformity and coating efficiency in a Bohle Lab-Coater using oval tablets. Eur. J. Pharm. Biopharm. 56, 3–9.
Tobiska, S., Kleinebudde, P., 2003b. Coating uniformity: influence of atomizing air pressure. Pharm. Dev. Technol. 8, 39–46.
Turton, R., 2008. Challenges in the modeling and prediction of coating of pharmaceutical dosage forms. Powder Technol. 181, 186–194.
Turton, R., 2010. The application of modeling techniques to film-coating processes. Drug Dev. Ind. Pharm. 36, 143–151.
Wadell, H., 1935. Volume, shape, and roundness of quartz particles. J. Geol. 43, 250–280.
Wilson, K.E., Crossman, E., 1997. The influence of tablet shape and pan speed on intra-tablet film coating uniformity. Drug Dev. Ind. Pharm. 23, 1239–1243.
Yamane, K., Nakagawa, M., Altobelli, S.A., Tanaka, T., Tsuji, Y., 1998. Steady particulate flows in a horizontal rotating cylinder. Phys. Fluids 10, 1419–1427.
Yamane, K., Sato, T., Tanaka, T., Tsuji, Y., 1995. Computer simulation of tablet motion in coating drum. Pharm. Res. 12, 1264–1268.
Zhou, Y.C., Xu, B.H., Yu, A.B., Zulli, P., 2002. An experimental and numerical study of the angle of repose of coarse spheres. Powder Technol. 125, 45–54.
Zhu, H.P., Zhou, Z.Y., Yang, R.Y., Yu, A.B., 2007. Discrete particle simulation of particulate systems: theoretical developments. Chem. Eng. Sci. 62, 3378–3396.
Zhu, H.P., Zhou, Z.Y., Yang, R.Y., Yu, A.B., 2008. Discrete particle simulation of particulate systems: a review of major applications and findings. Chem. Eng. Sci. 63, 5728–5770.